How the axial flux of an induction motor can be used?

Janusz Petryna *

Cracow University of Technology, ul. Warszawska 24, Krakow 31-155, Poland

Article history:
Received 10 June 2019
Received in revised form
13 July 2019
Accepted 13 July 2019
Available online 13 July 2019

Abstract
The article contains the results of research within the project to apply unipolar (axial) flux to obtain diagnostic signals carrying the information of: electrical asymmetries of machinery (inter-turn stator short-circuits, cage damages); rotational speed of the rotor and load torque. Inter-turn stator short-circuits can be detected both at starting process time (when they appear most often), as well as in steady states. Detection of rotor cage defects in steady states has a character of a comparative study, and over time, as the defects develop. For standard drives that are powered from the network and work in open systems, by measuring the voltage following a unipolar flux, it is possible to make measurement and recording of motor speed, which usually is almost never provided under industrial conditions. The study shows that a simple in its construction, cheap coil can be a very useful diagnostic tool. The measurements were carried out at the laboratory and motor workplace in the power plant, while in the test station, during the loading, characteristics illustrating the dependence of the torque on the axial flux and on the rotational speed were obtained. A way of using a single measurement to estimate the torque has been proposed. The method is relatively simple to implement and allows for a fully non-invasive determination of the load torque.

Keywords: axial flux, rotor cage damage, inter-turn short circuits, load torque, rotational speed measurement, induction motor, testing station, contactless measurements

1. Introduction

The issues of using axial flux of AC machines in diagnostics and exploitation have been present in research and many publications since quite a long time [1], [2], [3], [5], [8]. For some time, there has also been an interest in this subject from industry [11], [14], [15]. The measurement of the axial flux is easy to implement. A simple coil applied to the fan side of the working machine is enough here [19]. Machines normally powered from the network and working in open systems are almost never armed with instruments to measure and record changes in the speed and load torque. When a need to carry out such studies arises , a measuring coil can be used to capture the flux from the motor outside, enabling the observation of speed, load torque and diagnostic symptoms after an appropriate signal processing [18], [20]. The same information can be obtained from the axial flux signal as from the commonly used so far stator current time signal and stator current spectrum analysis but in much easier and comfortable way.

The study will analyze an application of measurement system based on axial flux and methodology of faults diagnosing and speed and load torque determination.

*Corresponding author: janusz.petryna@gmail.com

2. Method of axial flux acquisition

Every AC machine produces magnetic field inside and around its body. Fig. 1 shows the simplified view of magnetic flux distribution in and around an induction motor. For measurement purposes, components such as the axial flux along the shaft, also called the unipolar one, and the flux around the endwindings, are particularly useful.

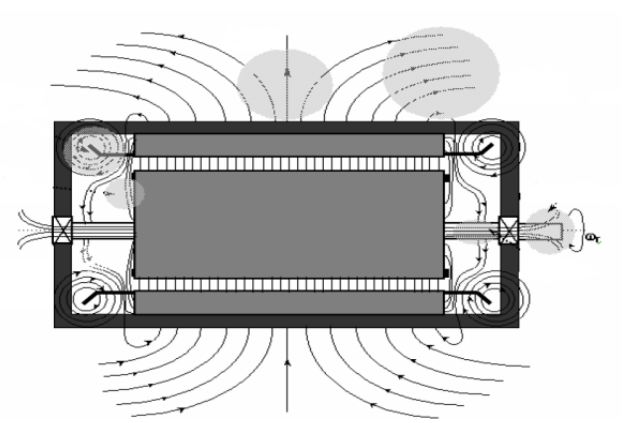

Figure 1. Flux distribution in an induction motor

The main tool in the process of flux acquisition is a measuring coreless coil with a great number of thin turns (10–15 thousands). The coil should be placed as close to the motor anti-drive

side as possible (Fig. 2–4). It should be noted that in every next measurement the distance and placing of the coil should be the same. The best solution providing repeatable conditions of measurements is mounting the coil inside the bearing lid (for machines with rolling bearings). The strength of the flux signal depends on a distance from the machine [5].

Figure 2. The method of measuring an axial flux at the work place – a coil on a tripod

Figure 3. The axial flux measuring coil mounted during testing of a large machine

The location of the measuring coil on the motor anti-drive side with the standard ribbed housing structure does not raise any objections. In the case of HV machines closed in a steel casing (Fig. 4), some have doubts as to whether a useful flux is able to penetrate into the air at all. Fig. 5 is a clear proof that it is so.

As it can be seen, despite of the steel casing, the axial flux of the motor gets thru and is recorded. The recorded signal can be subjected to low pass filtering in order to check the rotor starting cage condition and to FFT transformation to diagnose the working cage.

Figure 4. View of the stand for measuring high power HV machines with axial flux measurement

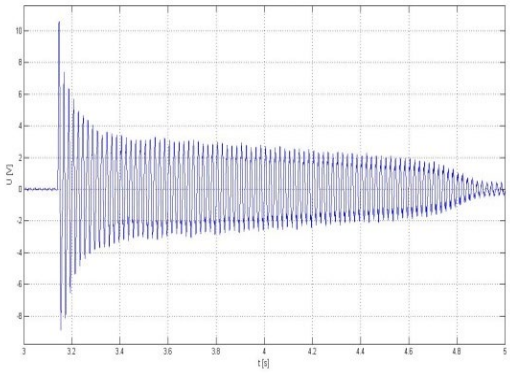

Figure 5. The measuring coil output voltage recorded outside the steel casing of the 6 kV 850 kW motor as in Fig.4 during the start-up

3. The application of an axial flux to a non-invasive diagnostics

The analysis of the axial flux signal time course and spectrum makes it possible to diagnose:
– rotor windings condition,
– rotor eccentricity
– and short-circuit faults and insulation weakening in the stator windings.

3.1.Diagnosing motor during start-up

Figure 6 presents the axial flux changes during the refrigerator fan motor start-up operation.

Table 1. Motor 1 data

Motor duty	Refrigerator fan
Power (kW)	30/132
Supply voltage (V)	400
Speed (rpm)	740/1485

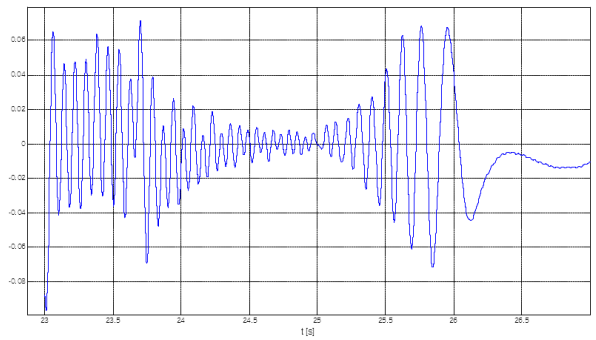

Figure 6. Low pass filtered axial flux time course during motor 1 start-up

A similar process for the water pump motor is shown in Fig. 7.

Table 2. Motor 2 data

Motor duty	Water pump
Power (kW)	840
Supply voltage (V)	6000
Speed (rpm)	2989

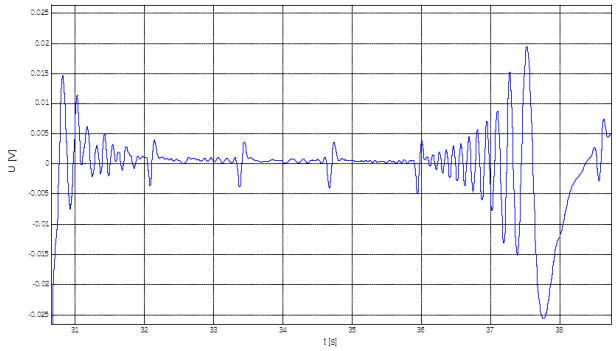

Figure 7. Low pass filtered axial flux time course during motor 2 start-up

Characteristic modulations in the flux signals of both motors 1 and 2 indicate damages of the rotor cages, their amplitudes increase as the defect range increases. For comparison, below Fig. 8 shows changes in the current during a motor start-up with a rotor cage defect.

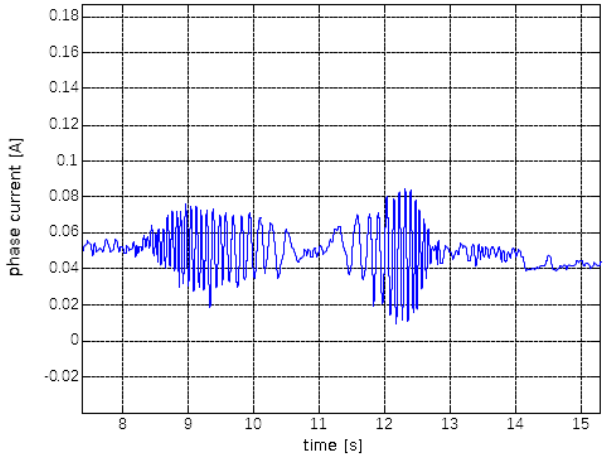

Figure 8. Low pass filtered **stator current** time course during motor start-up

3.2. Diagnosing in the steady state

One of the possibilities is to analyze the spectrum of the flux. The FFT analysis of the axial flux is similar to the current analysis method MCSA (Motor Current Signature Analysis). The first step in the spectrum analysis is to determine the motor speed – the basic parameter in the spectrum analysis. The flux spectrum contains information about the motor speed:

sf_0, f_r and $f_0(1\text{-}s)/p$ components, where f_0 – supply basic frequency, s – rotor slip, f_r – rotational frequency, p – motor poles pairs number.

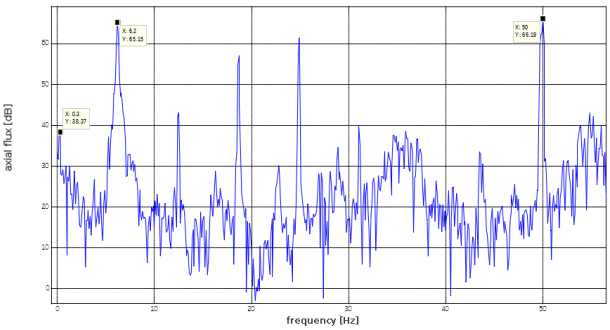

Figure 9. Basic components of the axial flux for speed determination (motor 3,7 MW, 10kV, 372 rpm) – spectrum range 0–60 Hz

The motor speed can be calculated by the formulas:

$$n = 60 f_0(1\text{-}s)/p = 60(f_0 - f_2)/p \quad (1)$$

where $f_2 = sf_0$ – rotor current frequency

Rotor winding problems

In case of the damage to the rotor cage, in the signal spectrum characteristic frequencies appear:

$$f_{ax\,bar} = (1-2s)f_0 \quad (2)$$
$$f_{ax\,bar} = (3-2s)f_0 \quad (3)$$
$$f_{ax\,bar} = (5-4s)f_0 \quad (4)$$

and generally

$$f_{ax\,bar} = kf_0 - l2sf_0 \quad (5)$$

The degree of the rotor winding degradation is determined by the RFI (Rotor Fault Index) factor, whose basic form has the following structure:

$$RFI = \frac{\max(A_1, A_2)}{A_0} \cdot p \quad (6)$$

where: A_1, A_2 – amplitudes of slip harmonics calculated from above the noise level; A_0 – amplitude of basic supply harmon-

ic calculated from above the noise level; p – motor poles pairs number

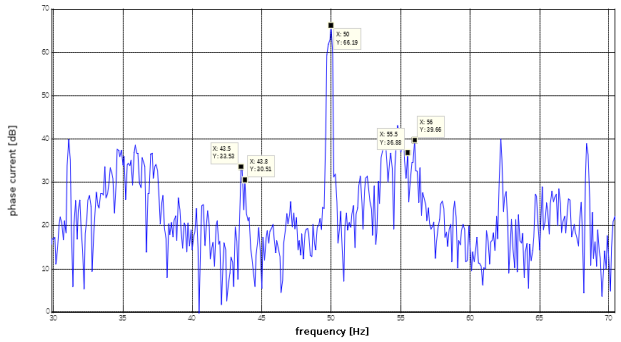

Figure 10. The axial flux spectrum for the 3,7 MW, 10kV, 372 rpm motor with marked frequencies of the largest slip components 43.8 and 55.5Hz, 100% load

In the Fig. 10 the marked sidebands indicate a serious problem in the rotor cage: a possible bar damage and overlapping load influence.

Fig. 11 shows a final result of rotor cage degradation: from high resistance joints of bars and end ring connections up to the crack of the ring. This is a severe damage which eliminates the motor from service.

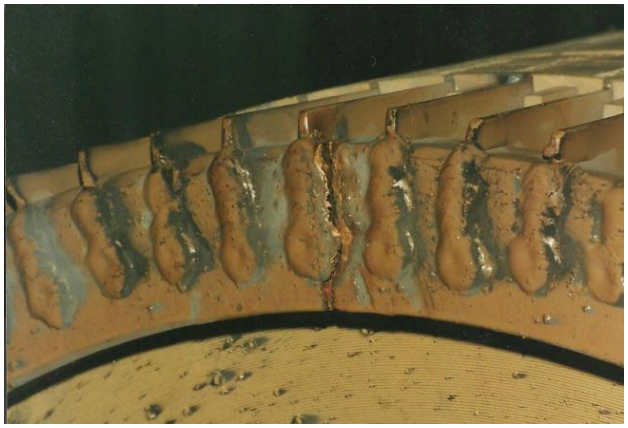

Figure 11. Broken end ring of the 800 kW, 6 kV, 745 rpm induction motor with RFI=2.15

Figures 12 and 13 show similarity of current and axial flux spectra (motor 850 kW, 6 kV, 2989 rpm).

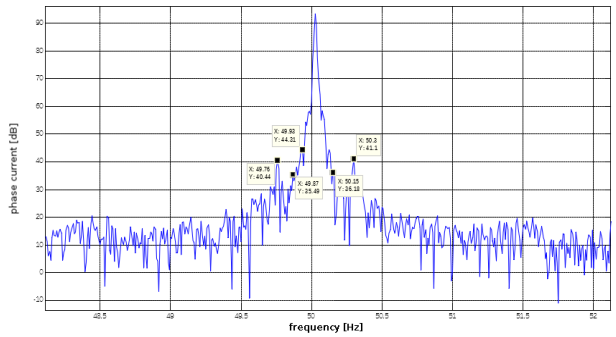

Figure 12. The current spectrum of the 6 kV 850 kW motor in steady state with marked characteristic components for the diagnosis of the rotor

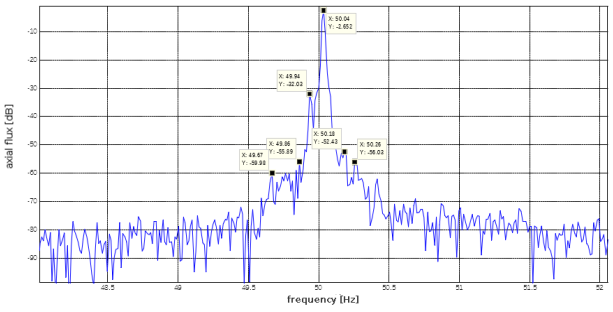

Figure 13. The axial flux spectrum of the 6 kV 850 kW motor in steady state with marked characteristic components for the diagnosis of the rotor

The RFI factor was evaluated based on both above current and axial flux spectra.

Table 3. RFI factors calculated on the basis of stator current spectrum and axial flux spectrum of motor 850 kW, 6 kV, 2989 rpm

	Current	Flux
RFI	0.333	0.320

Both the RFI coefficients for the current and flux spectra testify to the compatibility of both methods.

RMS axial flux voltage versus number of damaged rotor

In the laboratory of the Cracow University of Technology, several tests of 0.8 kW 220 V motors were carried out. Four identical SZJKe14 motors were tested: one healthy motor, three with damages to the rotor – 1, 2 and 3 broken bars, respectively. The view of the coil mounted on the housing of the tested motor is shown in Fig. 14.

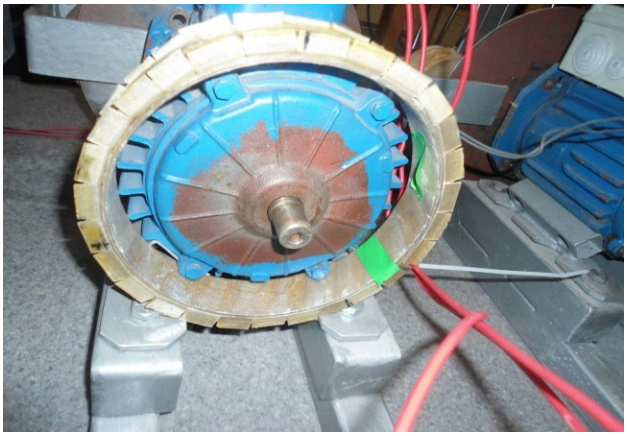

Figure 14. Tested motor with damaged rotor bars and measuring coil applied

The recorded signal directly from the coil was filtered by a lowband filter with a cut-off frequency of 10 Hz. Table 2 shows the effective values of the signal from the coil and the filtered signal. The filtered signal shows a clear dependence of the signal level on the number of damaged bars.

Table 4. Effective values of the signals vs. broken bars

Motor/Signal	Total [mV]	Filtered [mV]
Symmetric	42.7	1.3
1 broken bar	299.5	8.4
2 broken bars	301.5	9.7
3 broken bars	262.1	13.6

Another two three-phase squirrel cage 0.2 kW, 380 V motors: one healthy, the second with some broken bars, were subjected to tests. The coil was applied to the non-drive side of the motors. Figures 15 and 16 show the differences in the level of axial flux of both motors in the steady state. The damaged motor shows a signal level 7.5 times larger than a healthy one.

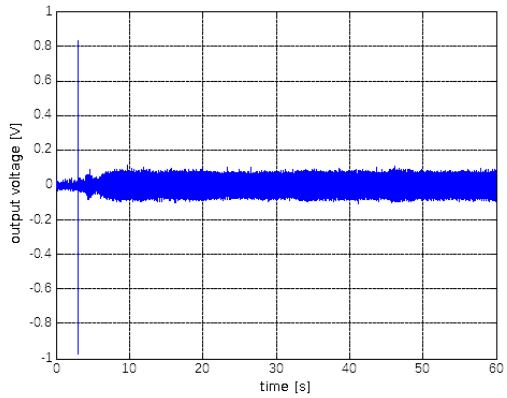

Figure 15. Time course of axial flux – healthy motor

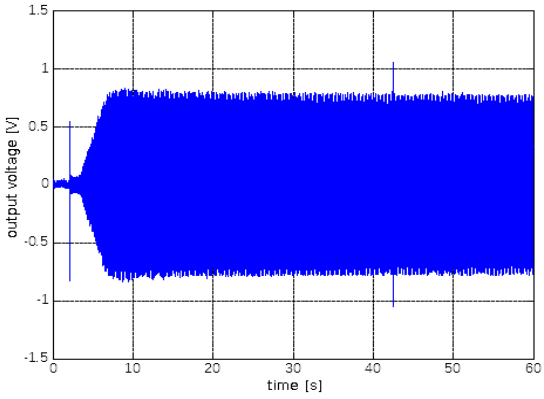

Figure 16. Time course of axial flux – damaged motor

3.3. Detection of short-circuits and insulation weakening

Inter-turn faults in stator winding

The coils short-circuits change the distribution of spatial harmonics of induction in the air gap. In the axial flux, time harmonics can be detected that occur with the spatial harmonics of the magnetic field. In dense coils the voltage is induced, which is the reason for the flow of current limited only by the own impedance of the close-loop coils. The current flowing through dense windings is the source of pulsation of magnetomotive forces, which affect the spatial harmonics of the field [8]. Inter-turn short circuits produce harmonics of frequencies [4], [5], [8]:

$$f_{ax\,sc}=kf_0\pm n(1-s)f_0/p \quad (7)$$

or $$f_{ax\,sc}=kf_0\pm nf_r \quad (8)$$

where: f_0 – fundamental supply voltage frequency; f_r – rotor rotational frequency; k – time harmonic order of supply voltage

Testing of stator winding faults

A 4 kW, 380 V (Y) induction motor was designed for testing, whereby a controlled short-circuit of 2 winding turns in the stator phase was allowed. A coreless coil of about 500 turns wound with a thin wire which was used to capture and measure the axial flux, was applied to non-drive motor side (fan). After starting the motor, in the steady state, by means of a switch, the short-circuit loop covering 2 adjacent turns was alternately shorted and opened.

Figure 17. Winding of the motor prepared for the implementation of the shorting of the coil

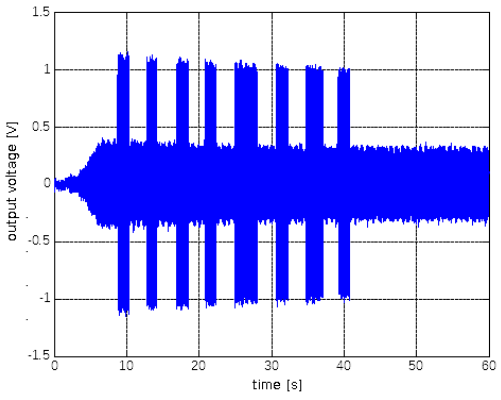

Figure 18. The voltage course in the measuring coil when shorting and opening 2 turns of the phase was realized

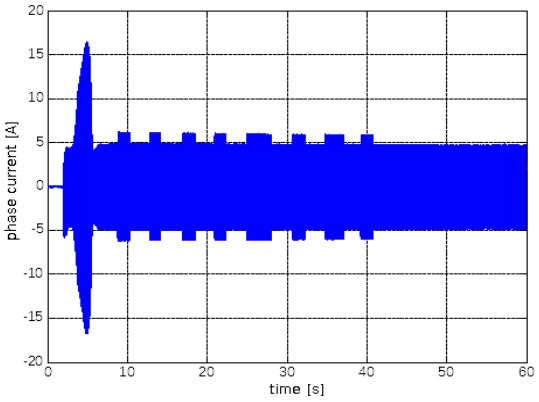

Figure 19. The course of the current in the phase where shorting and opening 2 turns of the stator was realized

Fig. 18 shows very distinct step change in the amplitude of the stream: triple in relation to the level before shorting. These changes were transfered to the phase current (Fig. 19) rather to a small extent. The amplitude of the phase current increased about 1.22 times, or by 22%. It should be added that the motor was running idle. Under load conditions, changes in current would be unnoticeable.

The measurement results are such that the measuring coil provides a strong, good quality signal, which indicates short-circuit faults of even a small number of turns, practically undetectable by current protections and that the measurement on the fan side (at first glance more difficult, because supposedly disrupted by rotating blades) does its job well.

It can also be stated that the signal coming from the axial flux is a good and relatively reliable signal to trigger the protection reacting to the inter-turns faults, because the size of the peaks caused by short circuits are volts.

Generator winding insulation weakening

The research object was a synchronous generator induced by permanent magnets, with suspected insulation weakening or even inter-turn short circuits.

To detect possible inter-turn faults, the measurement of the axial flux deriving from the windings inside the stator in the axis of symmetry of the machine was performed. During the tests, the stator of the machine was fed with a reduced voltage from the autotransformer, forcing about 40A in the windings for various phase associations.

When supplying the windings separately, the voltage signals were recorded for each phase U, V, W with effective values: 0.31V, 0.46V and 0.47V respectively. In this case, the signal in the first phase U was slightly different from the other voltage values for phase V and W.

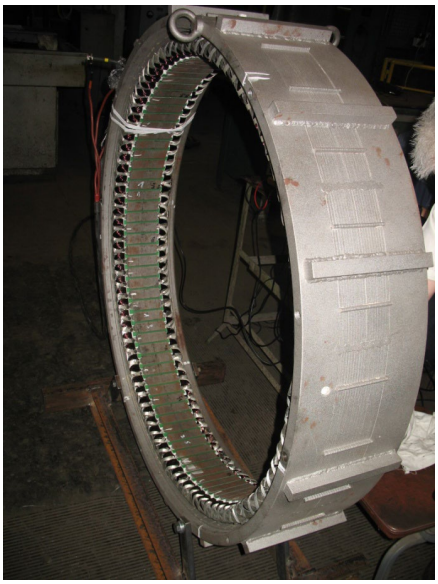

Figure 20. View of tested generator stator

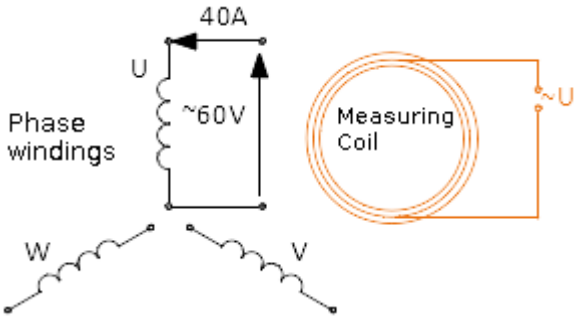

Figure 21. Power supply of individual phases after disconnection

When supplying the windings associated in the star connection, the results of measurements of the signal from the coil output placed inside the stator in its axis of symmetry were: for the U-V phases the coil output voltage was 0.16V, for the V-W phases the coil output voltage was 0.16V, for the W-U phases the coil output voltage was 0.01V. Conclusion: possible short circuit somewhere in a slot where the coils of two different phases W and U are placed together.

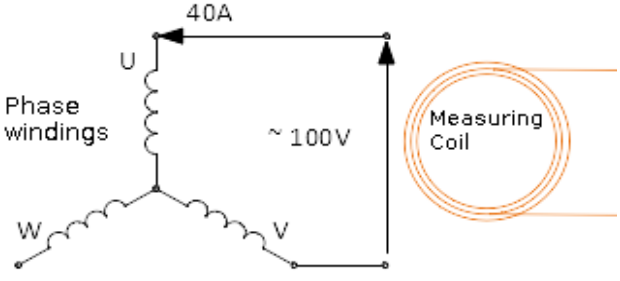

Figure 22. Power supply of every two connected phases

The result of the test prompted the service team to look for a possible short circuit. After removing the wedges, in one of the slots in which coils of 2 different phases meet, it was found a sign of damage to the insulation of both coils in the form of a short circuit caused by some tin drops.

3.4.Results of field calculations

It would be interesting to compare the above results with similar tests based on the 2D developed generator stator field model with use the JMAG program. Calculations were made for 2 cases: symmetry and the interphase inter-turn shorting in one slot. The calculations showed similar results of the magnetic field distribution inside generator stator.

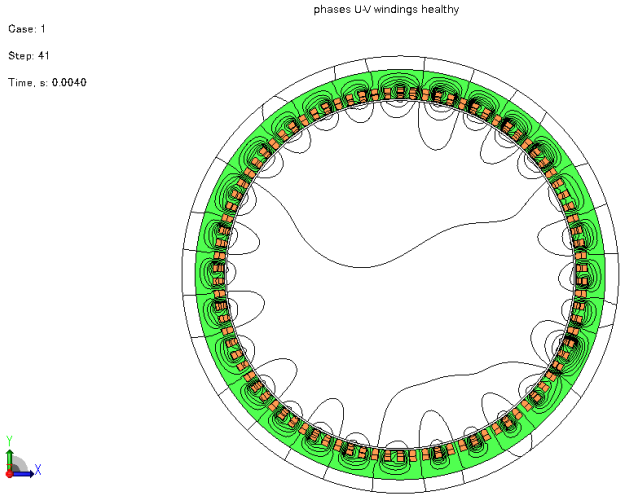

Figure 23. View of the stator cross section of the modeled generator in the JMAG program, flux distribution
a) electrical symmetry of the windings – magnetic flux present in the center of the stator

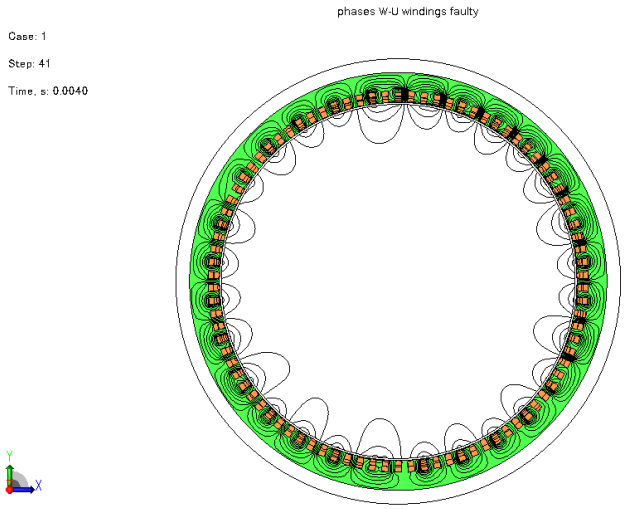

b) when supplying W-U phases – modeled phase-to-phase short-circuit in slot No. 1 – there is no flux in the center of the stator

4. The application of unipolar flux to non-contact determination of rotational speed, load torque and power and motor efficiency

4.1.Determination of rotational speed

In industrial conditions, the rotational speed of electric machines powered from the supply network is almost never recorded. If, however, for some reason the speed or the shaft torque are required, despite the lack of a tachogenerator or other device for measuring these quantities, they can be obtained based on the signal from the measuring coil applied outside the motor fan or non-drive side (Fig. 2, 3 and 4) or previously mounted inside the machine around the shaft or endwindings (Fig. 24).

Figure 25 shows the filtered waveform of the voltage from the coil, placed under the lid around the bearing on the 630 kW 6kV motor non-drive side.

The frequency of the waveform is equal to the changing frequency of the rotor current:

$$f_2 = sf_1 \quad (9)$$

so then

$$s = f_2/f_1 = T_1/T_2(t) \quad (10)$$

$T_1=1/f_1$, f_1 – frequency of stator current
$T_2=1/f_2$, f_2 – frequency of rotor current

Thus, the motor speed rpm can be expressed by:

$$n(t)=(60f_1/p)[1-s(t)]= (60/p)[f_1 - 1/T_2(t)] \quad (11)$$

Figure 24. 630 kW, 6 kV motor with built-in coil

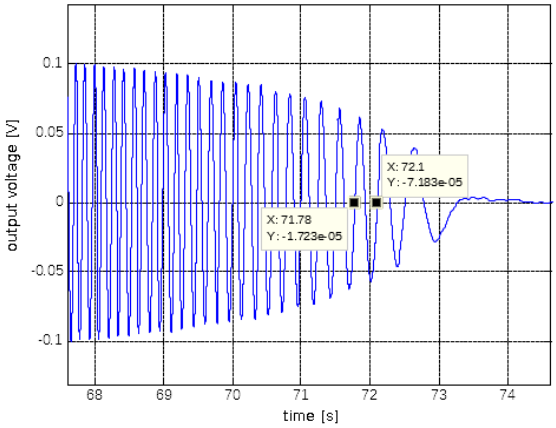

Figure 25. Filtered coil output voltage in the bearing lid corresponding to the rotor flux

For standard drives (powered from supply network, working in open-loop systems, without sudden changes of speed) the rotational speed measurement based on the axial flux seems to be sufficiently accurate.

4.2.Determination of the shaft torque

Research in the test room

Figure 26. View of the stand in Test Room

The motor was connected to the test bench and loaded in the range of 0.6 up to 1.2 nominal load. The measuring coil for the purpose to axial flux recording was applied to the fan side.

The characteristic of the effective voltage at the output of the coil deriving from the axial flux as a function of the load torque $U_\Psi = f(Tm)$ as in Fig. 27 was obtained. Fig. 28 shows inverted characteristics $Tm = F(U_\Psi)$. For this motor one just needs to have a coil and measure the motor flux to get the value of load torque directly from the characteristics from Fig.28.

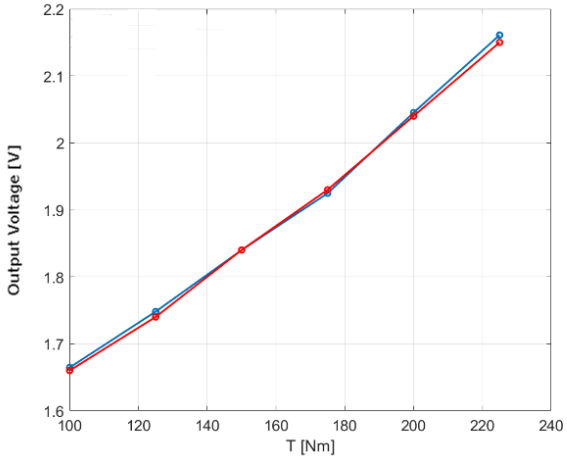

Figure 27. The effective voltage deriving from the axial flux as a function of the load torque

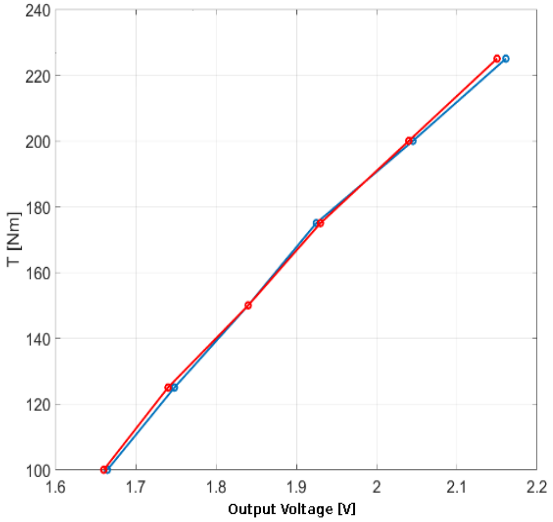

Figure 28. The load torque as the function of the axial flux – inverted characteristics

Also, on the basis of the dedicated measurement system, in which the voltage signal from the coil is processed directly into rotational speed (chapter 3.1, formula 11), the speed vs. load curve $n = f(Tm)$ – the mechanical characteristic was obtained. Then the load torque can be directly read through the speed value as in the Fig. 29.

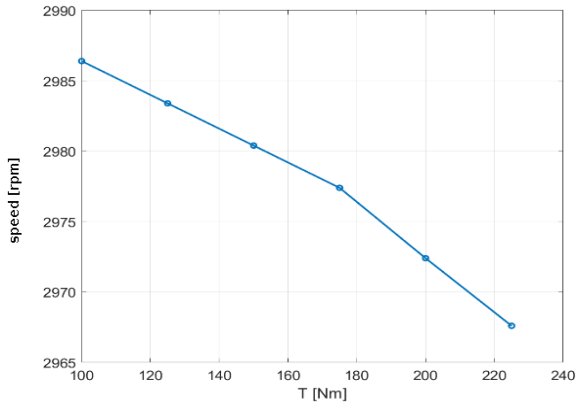

Figure 29. Motor speed as a function of the load torque

Measurement at the working place

Is it necessary to carry out tests in the test station for each motor operating in industry in order to obtain the characteristics $Tm = f(n)$ or $Tm = F(U_\Psi)$? That would be the best, but in practice it is not possible even for the most important machines in the installation. However, based on two points of motor operation on the installation: one measured and the other calculated in the range of typical loads – one can get a characteristic very close to the real one, which will enable reading the load torque with quite good accuracy.

Another words: enough is to make only one measurement of the motor axial flux with use of a coil which will lead to the motor speed determination and one read of motor supply voltage (which influences the actual torque), then on the basis of motor data to perform the calculation of the torque. In order to verify the calculated torque it might be necessary to read motor performance as voltages, currents and power in the switching room or control room.

The procedure as above was applied to the 1700 kW, 6 kV, 745 rpm motor. On the basis of axial flux voltage U_Ψ = 23,5 mV, the speed n = 747.5 – 747.6 rpm was read out from the spectrum (sf_0 component = 0.1583). Based on the speed the torque calculated was 12910 Nm.

To verify the calculated torque, the motor operation data were read in the switching room: supply voltage U=6381.6 V, phase average rms current I_{ph}=84 A, power consumed from the supply network P_1=1.034 *10^3 kW, power sent to the rotor:

$$P_\Psi = P_1 - 3R_s * I_{ph}^2 = 1.031 * 10^3 \text{ kW} \quad (12)$$

torque $$T = P_\Psi * (1 - s)/\omega = 9.55\, P_\Psi / n_0 = 13128 \text{ Nm} \quad (13)$$

The difference was 13128 – 12910 = 218 Nm, the error was -1.66%.

Having the torque calculated, it is easy to receive the load power:

$$P_2 = T * \omega = T * n / 9.55 \quad (14)$$

and the actual efficiency:

$$\eta = P_2 / P_1 \quad (15)$$

Conclusions

The article presents the applications of axial flux signal in diagnostics and operation of AC machines. The results of measurements and calculations presented here indicate the usefulness of the axial flux signal in both related fields.

By the way, it has been shown that a simple, cheap coil can be a very useful tool. It can be used as a sensor detecting without delay coil short-circuit, or as a device for measuring and comparing levels of degradation of the cage over time, and finally as an element of the system for measuring or recording rotational speed and torque on the motor shaft.

The presented research results encourage to take further, more advanced works also towards contactless determination of loads on induction motors, including the development of an on-line system enabling generation of the actual load torque value after entering basic motor data with an acceptable accuracy based on a single flux measurement.

This will allow, thus, the exact determination of machine efficiency and energy efficiency of the process and verify the technical condition of the installed devices.

References

1. P. Ewert "Use of Axial Flux in the Detection of Electrical Faults in Induction Motors", *IEEE International Symposium on Electrical Machines (SME)*, 2017, 1–6.
2. D.G. Dorrell, W.T. Thomson, S. Roach "Analysis of airgap flux, current, and vibration signals as a function of the combination of static and dynamic air-gap eccentricity in 3-phase induction motors", *IEEE Transactions on Industry Applications*, 1997, 33(1), 24–34.
3. V. Kokko "Condition monitoring of squirrel-cage motors by axial magnetic flux measurements", Academic Dissertation, University of Oulu, 2003, Finland
4. L. Gołębiowski, M. Gołębiowski, M. Noga, J. Skwarczynski "Axial flow in 3D FEM model of induction machine", *Elektrotechnika i Elektronika,* Vol. 25, No. 2, 147–152, 2006.
5. K. Chmelík, J. Foldyna, S. Mišák "Magnetické pole vokolí asynchronního stroje, jeho zjišťování *a* využití", *Electroscope*, č. 2. Západočeská univerzita v Plzni, Fakulta elektrotechnická, 2007.
6. Bobon "3D Finite Element Computation of Axial Flux in Induction Motor", *Transactions on Electrical Engineering*, vol. 1 (2012), No. 3 A247, 72–75.
7. W. Pietrowski "Wavelet analysis of axial flux in an induction machine on no-load test", *Electrical Review*, Vol. 88, No. 7b/2012, 20–23, 2012.
8. W. Jarzyna "Diagnostic characteristics of Axial Flux in an Induction Motor", *Seventh International Conference on Electrical Machines and Drives*, 1995 (Conf. Publ. No. 412), 141–146.

9. J. Tulicki, M. Sułowicz, J. Petryna "Application of the 2D field model to determine the axial flux signal for the purpose of diagnosing induction motors," *2017 18th International Symposium on Electromagnetic Fields in Mechatronics, Electrical and Electronic Engineering (ISEF) Book of Abstracts*, Lodz, 2017, pp. 1–2.
10. Petryna, J. Tulicki, M. Sułowicz "Calculating an electromechanical torque of a squirrel cage motor based on an axial flux obtained by the FEM", *II International Conference of Computational Methods in Engineering Science (CMES'17)*, 2017, ITM Web Conf., Volume 15, 1–8, 2017.
11. Frosini L., Borin A., Girometta, L., Venchi G.: *Development of a leakage flux measurement system for condition monitoring of electrical drives*. 2011 IEEE International Symposium on SDEMPED, 5–8 Sept. 2011, pp. 356–363.
12. Noga M., Petryna J.: *Dynamic states in induction machines with internal asymmetries*. TH Ilmenau Wiss. Zeitschr. 4/90
13. Keysan O., Ertan H.B.: *Higher Order Rotor Slot Harmonics for Rotor Speed & Position Estimation*. 12th International Conference on Optimization of Electrical and Electronic Equipment, OPTIM 2010, pp. 416–421.
14. Tulicki, J. Petryna, M. Sułowicz "Fault diagnosis of induction motors in selected working conditions based on axial flux signals", *Technical Transactions*, Issue: 13. Electrical Engineering, Issue: 3-E, 99–113, 2016.
15. Z. Ławrowski, A. Duda, J. Petryna, M. Sułowicz „Wyznaczanie momentu obciążenia silnika indukcyjnego w oparciu o pomiar strumienia poosiowego", *Zeszyty Problemowe - Maszyny Elektryczne,* nr 110, 1–8, 2016.
16. M. Sułowicz, J. Tulicki, J. Petryna, A. Duda „Wpływ uszkodzeń silnika indukcyjnego na dokładność bezkontaktowego wyznaczania momentu elektromagnetycznego z sygnału strumienia poosiowego", *Zeszyty Problemowe - Maszyny Elektryczne,* nr 119, 197–203, 2018.
17. J. Petryna, M. Sułowicz, A. Duda „Wykorzystanie strumienia poosiowego do badania stanów dynamicznych maszyn indukcyjnych małej i dużej mocy" *Zeszyty Problemowe – Maszyny Elektryczne,* Nr 2/2014 (102), str. 165–171
18. J. Petryna, M. Sułowicz, Ł. Puzio, A.Dziechciarz „Wykrywanie zwarć zwojowych w maszynach elektrycznych na stacji prób z wykorzystaniem cewki do pomiaru strumienia poosiowego" *Zeszyty Problemowe – Maszyny Elektryczne,* Nr 2/2015 (106), str. 185–190.
19. J. Petryna, M. Sułowicz, A. Duda, K. Guziec „Wykorzystanie strumienia unipolarnego w diagnostyce maszyn prądu przemiennego" *Zeszyty Problemowe – Maszyny Elektryczne,* nr 2/2013(99), 85–90.
20. J. Petryna, M. Sułowicz, A. Duda, Z. Ławrowski, K. Guziec „Bezkontaktowe wyznaczanie momentu obciążenia silnika indukcyjnego na stanowisku pracy w energetyce w oparciu o pomiar strumienia poosiowego" *Maszyny Elektryczne – Zeszyty Problemowe ,* Nr 2/2019 (122), 87–90.